VIBRATIONAL STABILITY OF PRE-MAIN SEQUENCE STARS

A THESIS SUBMITTED TO
THE GRADUATE SCHOOL OF NATURAL AND APPLIED SCIENCES
OF
THE MIDDLE EAST TECHNICAL UNIVERSITY

BY

MEHMET BURHAN

IN PARTIAL FULFILLMENT OF THE REQUIREMENTS FOR THE DEGREE OF

MASTER OF SCIENCE

IN

THE DEPARTMENT OF PHYSICS

JANUARY 2004

Approval of the Graduate School of Natural and Applied Sciences.

Prof. Dr. Canan Özgen
Director

I certify that this thesis satisfies all the requirements as a thesis for the degree of Master of Science.

Prof. Dr. Sinan Bilikmen
Head of Department

This is to certify that we have read this thesis and that in our opinion it is fully adequate, in scope and quality, as a thesis for the degree of Master of Science.

Prof. Dr. Halil Kırbıyık Co-Supervisor	Prof. Dr. Nilgün Kızıloğlu Supervisor

Examining Committee Members

Prof. Dr. Halil Kırbıyık	
Prof. Dr. Nilgün Kızıloğlu	
Prof. Dr. Ümit Kızıloğlu	
Assoc. Prof. Dr. Rikkat Civelek	
Assoc. Prof. Dr. Berahitdin Albayrak	

ABSTRACT

VIBRATIONAL STABILITY OF PRE-MAIN SEQUENCE STARS

BURHAN, MEHMET

M.S., Department of Physics

Supervisor: Prof. Dr. Nilgün Kızıloğlu

Co-Supervisor: Prof. Dr. Halil Kırbıyık

January 2004, 60 pages.

In this study, vibrational properties and stability of δ-Scuti like pulsating pre-main sequence stars have been investigated.

Studies were held in the mass range 2-4$M_{\odot}$ and limited to radial linear adiabatic pulsations. Numerical computations were performed by the oscillation program written by Kırbıyık & Al-Murad (1993). The models were selected to be at the latest phases of the pre-main sequence evolution where the luminosity starts to increase.

We have limited our calculations upto the end of the radiative inner regions, since at the surface of the star, our adiabatic perturbation computation does not perfectly fit to the relatively thin non-adiabatic convective envelope of the star. The results of the stability analysis showed that the PMS models undergo an instability whose time period is a function of mass.

Instability Strip of pulsating PMS stars was re-drawn with comparison to M. Marconi & F.Palla (1998). The effect of gravitational contraction on stability was also investigated.

Keywords: Pulsating Stars, PMS Evolution, Stability, Instability Strip

ÖZ

ANA-KOL ÖNCESİ YILDIZLARIN TİTREŞİM KARARLILIĞI

BURHAN, MEHMET

Yüksek Lisans, Fizik Bölümü

Tez Yöneticisi: Prof. Dr. Nilgün Kızıloğlu

Ortak Tez Yöneticisi: Prof. Dr. Halil Kırbıyık

Ocak 2004, 60 sayfa.

Bu çalışmada, δ-Scuti benzeri salınım yapan ana-kol öncesi yıldızların, titreşim özellikleri ve kararlılığı araştırılmıştır.

Çalışmalar, 2-4$M_{\odot}$ kütleleri için yapılmış ve çapsal lineer adyabatik salınımlarla sınırlandırılmıştır. Sayısal hesaplamalar Kırbıyık & Al-Murad (1993) tarafından yazılan programla yapılmıştır. Modeller, parlaklığın artmaya başladığı, ana-kol öncesi evrimin son safhalarında seçilmiştir.

Adyabatik pertürbasyon hesaplarımız, yıldızın daha ince adyabatik olmayan dış kısmına uymadığı için, hesaplamalarımızı ışınımsal iç kısmın sonuna kadar sınırlandırdık. Kararlılık analizinin sonuçları bize, ana-kol öncesi yıldızların, kütlesine bağlı bir uzunlukta kararsızlık yaşadığını göstermiştir.

Salınım yapan ana-kol öncesi yıldızların kararsızlık şeridi M.Marconi & F. Palla (1998) ile karşılaştırılarak yeniden çizilmiştir. Çalışmada, kütleçekimsel

çekilmenin kararsızlığa etkisi de incelenmiştir.

Anahtar Kelimeler: Zonklayan yıldızlar,Ana-Kol Öncesi Evrimi, Kararlılık, Kararsızlık Şeridi

TO MY SWEET FAMILY

ACKNOWLEDGMENTS

It is more than a thank what I should give to my supervisor Prof. Dr. Nilgün Kızıloğlu, not only for her invaluable guidance during this study, also for her praiseworthy patience. It has been a great pleasure to work under her supervision.

I would also like to thank Prof. Dr. Halil Kırbıyık for his helpful ideas and supports, for teaching me this subject and for being a model for me with his politeness.

But nothing compares with the confidence of the feeling of knowing that you have a great family who always prays for your health and success.

TABLE OF CONTENTS

LIST OF TABLES

TABLE

LIST OF FIGURES

FIGURE

CHAPTER 1

INTRODUCTION

1.1 Evolution of Pre-Main Stars (PMS)

Stars begin their billions of years of journey as an interstellar cloud spanning tens of parsecs across. Star formation begins when gravity begins to dominate over heat, causing a cloud to lose its equilibrium and start to contract. Not only the heat, also rotation and magnetic forces as well are barricade factors against contraction.

This pre-star is so low-dense that the photons produced can easily escape with a less number of absorption. This largeness in the star's size causes tremendous amounts for the luminosity comparing with its main sequence case as can be easily seen by the equation below:

$$L = 4\pi R^2 . F_T$$

where L=total luminosity, F_T=total flux, R=radius

In this stage the star is almost fully-convective which means the energy that mostly produced with the result of gravitational contraction is transfered to the surface of the star by convection. A star or a region in a star is said to be radiative

or convective with the help of Schwarzshild criterion; that is, the convective energy transport sets in if the radiative temperature gradient is greater than the adiabatic temperature gradient , otherwise, the star is in radiative equilibrium.

$\nabla_{rad} > \nabla_{ad}$ convective region

$\nabla_{rad} < \nabla_{ad}$ radiative region

where ∇ 's are the temperature gradients as follows;

$$\nabla_{ad} = (\frac{dlnT}{dlnP})_{ad} = (1 - \frac{1}{\gamma}) \tag{1.1}$$

$$\nabla_{rad} = (\frac{dlnT}{dlnP})_{rad} \tag{1.2}$$

where γ is the ratio of specific heats c_p to c_v which are the specific heats per unit mass at constant pressure and constant volume, respectively.

It will be usefull to define convective temperature gradient as well, for further approximations:

$$\nabla_{con} = (\frac{dlnT}{dlnP})_{con} = \nabla_{ad} + \nabla'_{con} \tag{1.3}$$

where ∇'_{con} is the super-adiabatic contribution to the convective temperature gradient.

The calculations assumed that stars begin this contraction as fully convective objects, with radii nearly two orders of magnitude larger than their final, ZAMS values (Iben 1965; Ezer & Cameron 1967). However such large radii could not have been attained during the previous protostar phase, when the stars were gathering mass from their parent interstellar clouds (Larson 1969; Winkler & Newman 1980; Stahler, Shu & Taam 1980).

The protostar moves down in the H-R Diagram as it gets smaller in radius and luminosity travels almost a vertical path what we call the Hayashi track. And all through this path, the star is taken into account in convection treatment.

In the early stages of PMS evolution, various rapid dynamical and thermal processes occur which modify the internal structure of the protostar. By the time the protostar reaches the classical instability strip on its way toward the main sequence, these complex phenomena have long dissapeared and the evolution has considerably slowed down. As contraction continues,the stellar matter starts to become denser,becoming more so as contraction proceeds. The protostar's internal heat gradually diffuses out from the hot centre to the cooler surface causing the overall contraction to slow down and when it reaches to the stage where the central temperature is enough to ignite nuclear reaction, protons begin fusing into helium nuclei in the core and the star is now said to be born.

At this stage, the star continues to contract a little more. But the luminosity begin to rise again as a result of nuclear contribution to the realesed energy. As the CNO cycle contribution becomes increasingly important and eventually dominant, the convective core slightly expands till ZAMS stage.

At the time the star reaches to the zero-age main sequence (ZAMS) where the pressure and gravity are finally balanced, hydrostatic equilibrium is achieved and nuclear energy can be considered as the sole energy source of the star. The zero-age main sequence is defined as the model with the minimum luminosity just before evolution starts back toward the red (Suran 2001).

The mass of the star determines how long it will be staying in the fully convective gravitationally contracting phase. The time, the star of 100 $M_{\odot}$ spends during the fully convective phase is only the order of a few tens of years while the 0.2 $M_{\odot}$ star reaches to the main sequence as a wholly convective star in 1.7x10^{9} years (Ezer 1967).

The fully convective phase is followed by a radiative stage for the stars in the mass range 100 $M_{\odot}$ to 0.3 $M_{\odot}$. Once the radiative core encompasses more than half of the stellar mass, the flux of energy is governed by the interior opacities. Since the opacities decrease with rising interior temperature and densities, during further contraction the luminosities show an increase. Therefore, the evolutionary track turns upwards. In the evolution of massive stars, it can be seen that the track becomes more and more horizontal. This is due to the fact that electron scattering is becoming the main source of the interior opacities. In stars with mass lower than 1Mo the growing radiative core cannot extend up to the surface.

In his study of comperative seismology of pre- and main sequence stars in the instability strip, Suran mentions about the structural and pulsational differences between pre- and main sequence stars of the same point on the H-R diagram: whereas PMS has some relics of its gravitational contraction phase, the main sequence nuclear burning modifies the inner core structure, and post-ZAMS models develop chemical inhomogenities. As expected the outer layers of associated models are very similar: density and temperature profiles and therefore the opacity profile are almost identical. On the other hand, the central regions significantly differ. A PMS model is slightly contracting and remains chemically

homogeneous. In contrast, a post-ZAMS model has a core which traces its nuclear history, changes its chemical composition and builds regions with μ gradients.

1.2 Pulsational Properties of PMS Stars

In our study we have dealed with the latest stages of PMS contraction when traces of formation phases have already disappeared, so that a PMS model can be built with quasi-static approximation.

The studies on pulsational properties of PMS stars have been focused mainly on the δ-Scuti pulsations of Herbig Ae/Be stars. The Herbig Ae/Be stars are pre-main sequence objects with masses ranging from 2 to 5 $M_{\odot}$ usually found within star formation regions. Mostly due to their dusty environment and active atmospheres and winds, they exhibit strong photometric and spectroscopic variability on timescales of few minutes to years indicating that photospheric activity begins in the earliest phases of stellar evolution prior to the arrival on the main-sequence (MS).

The fact that young stars, during their evolution to the MS move across the instability region of post-MS stars raises the possibility that at least part of these photospheric activities could also be due to stellar pulsations (Baade &Stahl 1989; Kurtz & Marang 1995). Noticeable studies were also held by M. Marconi & F. Palla (1998) and Suran et.al. (2001) and many others to clear out the pulsational properties of PMS type stars.

While having a study on PMS pulsations, we should take into account some other important characteristics of PMS stars that may be effective on pulsation

behind the active atmospheres. One is the star's contraction. L. H. Thomas (1931) [cf. P. Ledoux (1958)] stated that the entropy change of the quasi-equilibrium state around which the pulsation takes place may have important consequences to the excitation of pulsation. S. Kato and W. Unno (1967) worked out this problem and found that the contraction acts to excite the pulsation. In one of his studies on the pulsational instabilities of PMS stars, Isao Okamoto used pulsation-contraction coupling in the computation of the growth rate of pulsation which determines if the star is vibrationally stable or not (Okamoto 1967). He found that gravitational contraction has a considerable impact on the vibrational instability of his early PMS models.

The changing inner structure from convective to radiative in the time interval between early PMS phase and zero-age main sequence is another deterministic property of PMS stars. The inner, mostly radiative region is followed by a convective zone, with a size inversely proportional with the closeness to the zero-age main sequence. One can confidently apply adiabatic computitions for the central convective zones, but the convective outer regions of the stars always behave non-adiabatically. This can be easily seen by equation (1.3) since the super-adiabatic part of the convective temperature gradient is usually important in the outer layers of stars.

On the other hand as we shall see, the pulsational properties are quite sensitive to the structure of the outer layers. Among other things the depth of the outer convective zone will affect the period. As the cepheid calculations become more detailed and refined, it may possible to infer information about the outer zone

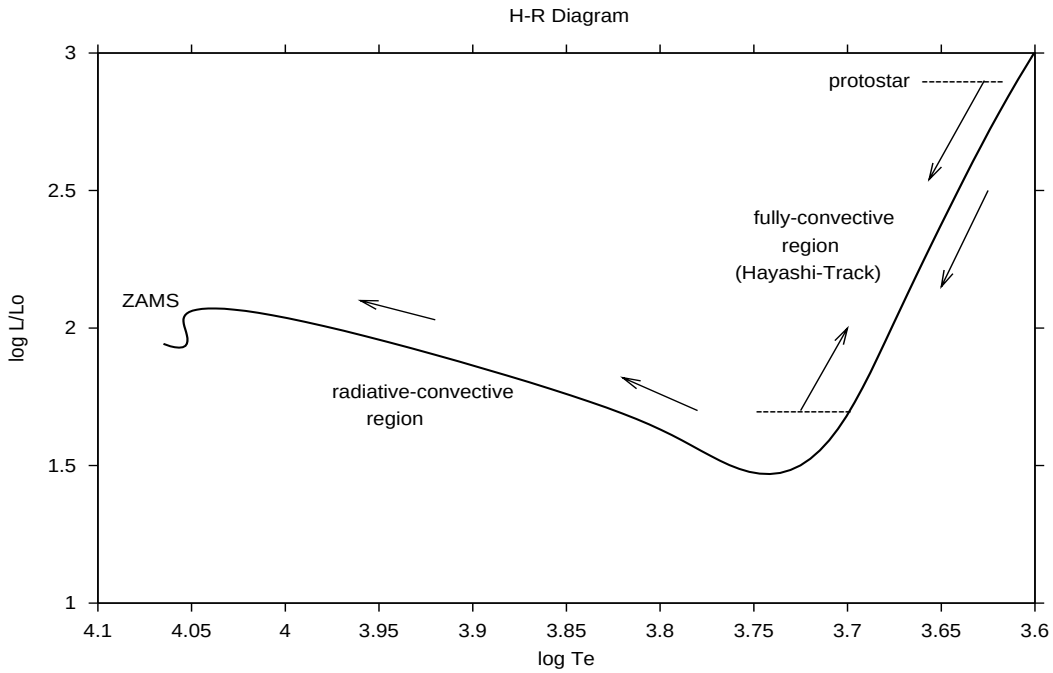

Figure 1.1: Pre-main sequence evolution

through a comparison of observed and calculated periods. Nor can we rule out the possibility that the structure of the convection zone may have a significant influence on the stability.

For a given mass and location in the H-R diagram, the frequencies of radial modes with same radial order remain nearly identical independent of whether it is a pre- or a post-ZAMS pulsator. As the outer layers in both stages are almost the same, oscillations in PMS stars should have the same level of amplitudes as in δ-Scuti stars; this means that some modes are expected to be detectable from ground.

Low radial order modes with dual (gravity and pressure) nature penetrate in the upper layers of the star and there is a good chance to observe them. Suran,

et al.(2001) have shown that we can use them as discriminators, as they are very sensitive to the structure of the inner layers, which is a deterministic difference between PMS and post-ZAMS stars. This might be particularly an interesting and useful method for this region of the H-R diagram where classical indicators of youth as disks or remaining nebulosities have dissapeared.

1.3 Observational Studies Over δ-Scuti Pulsations in PMS Stars

Observations of δ-Scuti like pulsations in PMS stars have mainly based on photometric studies. Breger (1972) was the first to report short term phometric variations resembling δ-Scuti pulsations in two PMS stars belonging to the young cluster NGC 2264: V 588 Mon and V 589 Mon. Although these results are based on the data obtained over a few hours on three nights seperated by several months, δ-Scuti pulsations are clearly suggested in these photometric variations, with frequences of 9.09 and 8.06 c/d, respectively. Only monoperiodicities were evidenced with considerable ambiguity on their reality and large uncertainities on their frequences, due to the limited amount of data.

Years later it was shown from photometric monitoring that δ-Scuti pulsations in the Herbig Ae star HR 5999 can be distinguished from the higher amplitude, longer timescale variations due to variable dust obscuraction or surface activity (Kurtz & Marang, 1995). Only one frequency at 4.8 c/d, was found in these data. Photometric data of HR 5999 from 9 years earlier were recently re-analyzed (Kurtz & Catala, 2001) and shown to exhibit the same mode. This indicates that pulsation modes in these stars can be stable over periods of at least a decade, and

that PMS stars, and in particular HR 5999, are excellent candidates for searching for mode frequency changes due to evolution of the star's internal structure, as already suggested (Breger & Pamyatmykh,1998). PMS evolutionary timescales are indeed short enough to yield relative variations of pulsation periods of the order of $P\cdot/P = 10^{-6}yr^{-1}$, which translate into drifts of about 0.4 hrs in 10 years for the timing of maxima in the light curve, and should be observable.

Photometric monitoring of PMS stars has recently led to the discovery of δ-Scuti pulsations in several of them. These results are summarized in Table 1.1 (table:Catala 2003, p56). Although still rather short, the list of PMS stars detected as δ-Scuti pulsators has increased noticeably in the last few years, after the existence and location of PMS instability strip was predicted, on the basis of stability analysis of the first three radial overtones (Marconi & Palla, 1998). Most of the stars presented in the Table 1.1 indeed fall within the instability strip, but many further observations of δ-Scuti pulsations in PMS stars are necessary to define observationally the boundaries of this instability strip.

Due to poor duty cycle and short time span of the observations performed so far, only monoperiodicities were detected in most cases, and a few reported multiperiodicities are still very uncertain. Besides, even if the measured frequencies indeed represent the actual stellar pulsation modes, these modes are not identified and can correspond to radial and non-radial pulsations.

The photometric studies of δ-Scuti pulsations in PMS stars are therefore still in a preliminary stage and can hardly be exploited astroseismologically, although various attempts have been made in this direction (Catala, 2003)

Table 1.1: Summary of photometric investigations of pulsations in PMS stars

Star	$\nu_1(c/d)$	$\nu_2(c/d)$	Sp. type	References
V 351 Ori	15.5	11.9?	A7	(Marconi et al., 2000,2001) (Balona et al., 2002)
V 346 Ori	34.2	21.2	A5	(Pinherio et al., 2002)
HD 104237	33.3	36.6?	A5	(Kurtz & Muller, 1999) (Donati et al., 1997)
HR 5999	4.81		A7	(Kurtz & Marang, 1995) (Kurtz & Catala, 2001)
HP 57	12.73	15.52		(Pigulski et al., 2000)
BL 50	13.91	9.89		(Pigulski et al., 2000)
V 588 Mon	9.1		A7	(Breger, 1972)
V 589 Mon	8.1		F2	(Breger, 1972)
HD 142666	21.4		A8	(Kurtz & Muller, 2001)
HD 35929	5.1		A5	(Marconi et al., 2000)

Several spectroscopic monitoring studies have been made on pulsating PMS stars but mostly complementary to photometry, and only be used to confirm the frequencies found in photometry. But the bright forthcoming strategy for observing these stars is being assumed to be the space-based investigations. Three ongoing astroseismology space projects; COROT (will be launched in 2005), MONS (will be launced in 2006) and EDDINGTON (will be launched in 2008) have the possibility of observing PMS stars as part of their programme. These future space-based astroseismology missions have the potential to provide very high quality seismic data for PMS stars.

CHAPTER 2

THE THEORY OF STELLAR OSCILLATION

2.1 Physics of a Pulsating Star

A pulsating (or an oscillating) star can simply be described as a star whose luminosity and radius change periodically with time. But beneath of all lies complicated but methodical structural changes within the star. All these variations occur when an auto-causal effect perturbs a zone to violate its equilibrium state. After that works the thermodynamic rules.

Every structural component of the star acts to relax itself and come back to equilibrium state. Relaxation of any infinitesimal element means the perturbation of its surrounding elements. This continuous actions happen to form a periodic movement of star's fluid.

The work done by each layer of the star during each pulsation cycle is the difference between the heat flowing in that layer and heat leaving it. The characteristics of the movement identifies whether it would be a radial or non-radial oscillation.

In radial oscillations these thermodynamic pulses move along the radius, vertical to the layers of the star. There is a spherical symmetric expanding or contracting of the star around an equilibrium position.

On the other hand, a non-radial pulsating star also has a horizontal component for the fluid velocity. A pulsating layer deviates from its initial shape with adaptation to the spherical harmonics with an order depending on the specific mode of oscillation.

Indeed, no matter if it is a radial or non-radial oscillation, all the physical parameters (ρ,T,P,r,...) are functions of the term $Y_l^m(\theta,\phi)\exp(-i\sigma t)$ where;

Y_m^l: spherical harmonics

σ: angular oscillation frequency

These l and m numbers define how the oscillation takes place. There are $\mid m \mid$ azimuthal and $l- \mid m \mid$ latitudal lines on the surface.

For example radial oscillation is just a specific case of non-radial oscillation with both l and $\mid m \mid$ is equal to zero means no horizontal lines on the surface.

These intersecting lines form consequent contracting and expanding regions which makes the non-radial oscillation.

We also have another quantum number, k (node number) that is the number of points in equilibrium when defining the mode of an oscillation. For example, k=0 state is fundamental mode, k=1 1st overtone, etc...

2.2 Propagation of the Waves

Two local frequencies are found in an oscillating medium, that are Lamb and Brunt-Vaisala frequency. Lamb frequency (L_l) is the frequency corresponding to the period which would be required for a sound wave to travel one horizontal length.

$$L_l^2 = \frac{l(l+1)c_s^2}{r^2} \tag{2.1}$$

where c_s is the adiabatic sound wave.

Brunt-Vaisala frequency is the frequency of a gas bubble oscillating vertically around its equilibrium position under gravity and can be expressed with;

$$N^2 = g(\frac{dlnP}{\Gamma_1 dr} - \frac{dln\rho}{dr}) \tag{2.2}$$

Propagation diagram is the plot of the oscillation frequencies of a star that shows the propagation of p-mode (pressure) and g-mode (gravity) oscillations and trapping regions.

In the region with $\sigma^2 > L_l^2, N^2$, oscillation behaves like an acoustic wave and the restoring force is due to the excess pressure while in $\sigma^2 < L_l^2, N^2$ region oscillation is just like a gravity wave and the restoring force is due to buoyancy.

In the other two regions with $L_l^2 > \sigma^2 > N^2$ and $L_l^2 < \sigma^2 < N^2$ the eigenfunctions decrease exponentially, so the oscillation amplitudes are trapped.

2.3 Excitation Mechanisms

It is quite sure that there should be an internal or external first touch to start all these to happen. We have a few number of excitation mechanisms in this manner. The two most common are ϵ- and κ-mechanisms. In $\epsilon-$mechanism, star's nuclear energy generation may have suddenly increase or decrease to excite the upper layers to ignite oscillation.

ϵ-mechanisms are not in use in PMS studies since these stars are weak nuclear energy generators or might have not begun generating at all.

κ-mechanism sets in when a relatively more opac region absorbs an excessive amount of heat. This absorption of heat enhances the local rate of temperature increase and causes the temperature and therefore also the pressure, to be slightly larger during the ensuing expansion that would be the case with adiabatic motion.

In the outer envelope in the radiative equilibrium, radiative flux is constant and the κ-mechanism works for driving an oscillation if,

$$\frac{d}{dr}(\kappa_T + \frac{\kappa_\rho}{\Gamma_3 - 1}) > 0 \tag{2.3}$$

where, κ_T and κ_ρ are opacity derivatives as $\kappa_T = (\frac{\partial ln\kappa}{\partial lnT})_\rho, \kappa_\rho = (\frac{\partial ln\kappa}{\partial ln\rho})_T$.

If a region in the stellar envelope satisfies this condition; radiative flux from the stellar interior is blocked by the effect of the temperature and density dependence of opacity. The blocked energy is converted to the energy of the oscillation.

2.4 Basic Equations

To reach a solution about understanding the behaviour of an oscillating star, we initiate our calculations with basic equations of hydrodynamics and heat flow. Perturbations are applied to the physical parameters of equilibrium structure which is formed by these equations and with the help of other stellar equations, the wave equation is reached with all the oscillation information within.

The basic equations are conservation of mass, momentum and energy:

$$\frac{\partial \rho}{\partial t} + \nabla.(\rho \mathbf{u}) = \mathbf{0}, \tag{2.4}$$

$$\rho(\frac{\partial}{\partial t} + \mathbf{u}.\nabla)\mathbf{u} = \rho\mathbf{f} - \nabla\mathbf{p} - \rho\nabla\mathbf{\Phi} + \nabla.\wp, \tag{2.5}$$

$$\rho T(\frac{\partial}{\partial t} + \mathbf{u}.\nabla)\mathbf{S} = \rho(\epsilon_{\mathbf{N}} + \epsilon_{\mathbf{v}}) - \nabla.\mathbf{F_R}, \tag{2.6}$$

where, ρ denotes density, p pressure, T temperature, $\mathbf{u}$ the fluid velocity, S the specific entropy, Φ the gravitational potential, $\mathbf{f}$ the electromagnetic and external forces, ϵ_N the nuclear energy generation rate, ϵ_v the viscous heat generation, F_R the radiative energy flux and $\wp$, the viscous heat generation.

Under stellar conditions we can generally ignore internal friction (or viscosity) in the gas and with the help of 1^{st} Law of Thermodynamics (dQ=TdS, Q=heat loss or gain of the system) we can rewrite the energy equation as follow:

$$\frac{dQ}{dt} = \rho\epsilon_N - \nabla.\mathbf{F_R} \tag{2.7}$$

These equations can be re-arranged for the effect of some specific conditions such as the inclusion of magnetic field or rotation. We assume the unperturbed

solution to be an equilibrium one, characterized by $\mathbf{v_o}$. Using time dependence ($\frac{\partial}{\partial t} = 0$), leads us to the equations of equilibrium state.

In order to linearize these equations we have to define mathematical descriptions for the physical perturbations and apply them to the equilibrium state. In this manner we should introduce two perturbation mechanisms:

Eulerian perturbation ('), deals with a given position within the star and observes the physical changes of that position while Lagrangian perturbation deals with a given fluid element and its physical changes.

$$f'(r,t) = f(r,t) - f_o(r,t) \qquad Eulerian\ perturbation \tag{2.8}$$

$$\delta f(r,t) = f(r,t) - f_o(r_o,t) \qquad Lagrangian\ perturbation \tag{2.9}$$

and the relation between them;

$$\delta f(\mathbf{r},\mathbf{t}) = \mathbf{f}(\mathbf{r},\mathbf{t}) + \xi \nabla \mathbf{f_o}(\mathbf{r},\mathbf{t}) \tag{2.10}$$

where, $\xi = \mathbf{r} - \mathbf{r_o} = \delta\mathbf{r}$

With these perturbations added to unperturbed states, the linearized, homogeneous equation set is formed. This is the point we are now involved in a perturbed star's dymamics.

$$\frac{\partial \rho'}{\partial t} + \nabla.(\rho_o \mathbf{v}) = \mathbf{0}, \tag{2.11}$$

$$\rho_o \frac{\partial \mathbf{v}}{\partial t} + \nabla p' + \rho_o \nabla \Phi' + \rho' \nabla \Phi_o = 0, \tag{2.12}$$

$$\rho_o T_o \frac{\partial}{\partial t}(S' + \xi.\nabla S_o) = (\rho \epsilon_N)' - \nabla.\mathbf{F}', \tag{2.13}$$

$$\nabla^2 \Phi' = 4\pi G \rho'. \tag{2.14}$$

The spherically symmetric assumption of equilibrium state makes it easier to use the spherical coordinates (r, θ, ϕ). The equations above may be reformed for two distinct components; radial and horizontal. Radial oscillation studies simply neglect the horizontal components. This gives;

$$\vec{\nabla} = \vec{\nabla}_r + \vec{\nabla}_\perp = \underbrace{\frac{\partial}{\partial r}\hat{r}}_{radial\ part} + \underbrace{\frac{1}{r}\frac{\partial T}{\partial \theta}\hat{\theta} + \frac{1}{r\sin\theta}\frac{\partial}{\partial \phi}\hat{\phi}}_{horizontal\ part} \tag{2.15}$$

2.5 Adiabatic Approach

Adiabatic assumption for an oscillating star means no heat gains or losses by the oscillating mass elements. Assuming the oscillations to be adiabatic is indeed unrealistic and an incomplete treatment because it yields no direct information regarding the thermal behaviour of the star. On the other hand, it does give quite accurate values for the pulsation periods and amplitudes of the star.

We assume the motion to be adiabatic ($\delta(\epsilon - \nabla.F/\rho) = 0$). For this treatment we can freely choose δS to be zero also. Manipulations with some other approximations take us to an eigenvalue problem with the eigenvalue σ^2.

$$\frac{1}{r^2}\frac{d}{dr}(r^2\xi_r) - \frac{g}{c^2}\xi_r + (1 - \frac{L_l^2}{\sigma^2})\frac{p'}{\rho c^2} = \frac{l(l+1)}{\sigma^2 r^2}\Phi', \tag{2.16}$$

$$\frac{1}{\rho}\frac{dp'}{dr} + \frac{g}{\rho c^2}p' + (N^2 - \sigma^2)\xi_r = -\frac{d\Phi'}{dr}, \tag{2.17}$$

$$\frac{1}{r^2}\frac{d}{dr}(r^2\frac{d\Phi'}{dr}) - \frac{l(l+1)}{r^2}\Phi' = 4\pi G\rho(\frac{p'}{\rho c^2} + \frac{N^2}{g}\xi_r). \tag{2.18}$$

Above equations are equivalent to a fourth order differential equation. Next thing to do is to find the corresponding boundary conditions for solving the problem. By applying some approximations at the center and surface, we find

the following boundary conditions:

$$\frac{d\Phi'}{dr} - \frac{l\Phi'}{r} = 0, \tag{2.19}$$

$$\xi_r - \frac{l}{\sigma^2 r}(\frac{p'}{\rho} + \Phi) = 0 \quad at\ center, \tag{2.20}$$

$$\delta p = 0, \tag{2.21}$$

$$\frac{d\Phi'}{dr} + \frac{(l+1)}{r}\Phi' = 0 \quad at\ surface. \tag{2.22}$$

As can be seen above, in adiabatic treatment knowing p(r),ρ(r),g(r) and Γ_1(r) is enough to determine the oscillation frequencies.

In high radial order or high degree modes Cowling approximation can safely be used, where the perturbation in the gravitational potential is neglected ($\Phi' = 0$)(Cowling, 1941). This is a commonly used approximation which directs the calculations to a Strum-Lioville type problem again with σ^2 being the eigen-value.

These equations were solved numerically under the Cowling approximation with proper boundary conditions and dimensionless variables by Kırbıyık & Al-Murad (1993) with the FORTRAN code which we have used to study the stability problem in the present thesis.

CHAPTER 3

VIBRATIONAL INSTABILITIES OVER RADIAL ADIABATIC PULSATIONS

3.1 Computation of Stability

The main purpose of studying vibrational stability is to discover the sources of instability which is responsible for the observed variabilities and find out which regions in a star are driving and which regions are trapping the oscillation.

In Chapter 1, we have mentioned about the behaviour of physical parameters of a pulsating star. In a general expression, these parameters vary exponentially with time. For example, for the radial perturbation:

$$\delta r \propto e^{(i\sigma_a - \sigma')t} \tag{3.1}$$

where, δr is the Lagrangian displacement of the point r, $\sigma_a/2\pi$ is the frequency of the oscillations and both are derived from the numerical solution of the Sturm-Liouville system of equations formed under radial adiabatic assumptions.

As can be seen from equation (3.1), for negative σ' (vibrational stability coefficient or growth rate), perturbed values will grow in time that makes the star

to be called as "vibrationally unstable". In such a case the star's expansion may not be balanced by the restoring mechanisms and some matter may be ejected from the outer parts in order to secure the stability.

"Instability Strip" is an expression for the time interval on H-R diagram during which the star undergoes a vibrationally unstable state. On the other hand, positive values of σ' make the oscillations trapped with time. The ratio $|\sigma'/\sigma_{ad}| << 1$ is always about the same order of the dynamical to thermal time scale ratio.

There exist a minimum value for σ^2 which, were we doing quantum mechanics, would correspond to the ground state.

The vibrational stability, as well as dynamical and thermal stability, is the problem of the exchange from one type of energy to another in a system. At this stage the work integral (W) should be introduced which is defined as the increase of the total energy E over one period of oscillation. For a nearly strictly periodic oscillation (i.e.,$\oint \delta T dt \cong 0$), W is given as (Eddington, 1926):

$$W = \oint dt \int_0^M \frac{\delta T}{T} \delta(\epsilon - \frac{1}{\rho}\nabla.F) dM_r \tag{3.2}$$

where $\oint dt$ indicates the integration over one period of oscillation and F is the flux radiated away from the mass element dM_r.

Several expressions can be in use for the work integral. For example the following presentation of W(r) by Baker and Kippenhahn (1962) is an accurate one but more convenient for linear non-adiabatic numerical calculations since adiabatic approximations reject the entropy change.

$$W = \oint dt \int p\mathbf{v}.d\mathbf{S}(r) = \oint dt \int_0^{M_r} \frac{1}{\rho}\nabla.(p\mathbf{v}) dM_r \tag{3.3}$$

As mentioned before, both of these expressions are applicable to the oscillation which is artificially enforced to be purely periodic. The main reason that makes the work integral fit for use is that we see where the excitation and damping zones are located in the stellar interior. If W(r) or dW/dr is plotted as a function of the position in the stellar interior, dW/dr is positive in an excitation zone and negative in a damping zone.

The growth rate $\sigma_I(\sigma')$(imaginary part of $\sigma = \sigma_R + i\sigma_I$) is derived from the work integral W as follows:

$$\sigma_I = -\frac{1}{2}\frac{W/E_w}{\pi} \tag{3.4}$$

where $\pi = 2\pi\sigma^{-1}$is the period,E_w is the total wave energy and expressed by:

$$E_w = \frac{1}{2}\sigma_R^2 \int_0^M \left|\vec{\xi^2}\right| dM_r \tag{3.5}$$

Combining all these, the overall expression of σ' can be written as:

$$\sigma' = \sigma_I = -\frac{1}{2\sigma_a^2}\frac{\int_0^{M_a}(\frac{\delta T}{T})(\epsilon - \frac{1}{\rho}\vec{\nabla}.\vec{F_R})dM_r}{\int_0^M \left|\vec{\xi^2}\right| dM_r} \tag{3.6}$$

It should be noticed that the integral on the numerator is taken up to the mass above which the adiabatic approximation ceases to be valid (Ledoux, 1965). This is because the Lagrangian perturbation of luminosity ($\delta L/L$) has already been calculated in adiabatic approximation. The outer envelope of a star has a short thermal time-scale, hence the non-adiabatic effect is large. So the integral is taken up to the radius which satisfies,

$$w\frac{\tau_{th}}{\tau_{dyn}} \approx 1 \tag{3.7}$$

where τ_{th} and τ_{dyn} are the thermal and dynamical time-scales, respectively.

σ' equation has a very simple physical meaning; positive contributions come from those part of the star that are heated at maximum compression and where therefore $\delta T/T$ and $\delta(\epsilon - \frac{1}{\rho}\nabla.F)$ have the same sign. In other words the star is driving pulsation if heat is absorbed ($dQ > 0$) when temperature is on increase ($\delta T > 0$) or heat is emitted when temperature is on decline.

The integral in the denominator is the oscillatory moment of inertia and has no influence on the sign of σ' since it is always positive.

After some manipulations over the Lagrangian variations relative to ρ and p and the pulsation period, σ_a areobtained from the adiabatic solutions of perturbation equations. The perturbed values for density and temperature are also accessible simply with the adiabatic approximation.

We have obtained the Lagrangian variations of ρ and p;

$$(\frac{\delta\rho}{\rho}) = \frac{1}{\Gamma_1}(\frac{\delta p}{p}), \tag{3.8}$$

$$(\frac{\delta T}{T}) = (\Gamma_3 - 1)(\frac{\delta\rho}{\rho}). \tag{3.9}$$

where Γ_1,Γ_3 is the adiabatic exponents;

$$\Gamma_1 = (\frac{\partial ln\rho}{\partial lnp})_s, \qquad \Gamma_3 = (\frac{\partial lnT}{\partial ln\rho})_s + 1 \tag{3.10}$$

For a star generating its own energy from the central nuclear reactions, the first term on the right-hand side of equation (3.2) demonstrates the effect of energy perturbation:

$$\delta\epsilon = \sum_{i,j}\sum_{i,j}(\mu_{ij}\frac{\delta\rho}{\rho} + \nu_{ij}\frac{\delta T}{T} + \frac{\delta X_i}{X_i} + \frac{\delta X_j}{X_j}) \tag{3.11}$$

The sum is carried over all reactions (i,j) taking place. X_i and X_j are the relative mass abundances of the reagents in reaction (i,j) and

$$\mu_{i,j} = (\frac{\partial log\epsilon_{i,j}}{\partial log\rho})_{X_i,X_j,T} \qquad \nu_{i,j} = (\frac{\partial log\epsilon_{i,j}}{\partial logT})_{X_i,X_j,\rho} \tag{3.12}$$

However, since the models we used have a negligible nuclear energy generation we can drop the first term. In PMS stars, this effect is being neglected thus the stability of the star is decided by the phase relations for the flux divergence. Instead of nuclear energy generation, we have studied the effect of gravitational energy generation which will be metioned in the following chapters.

The second term (flux term) on the right-hand side of equation (3.2) symbolizes the energy radiated away from the star thus it has a stabilizing effect. Expanding this term;

$$\frac{1}{\rho}\vec{\nabla}.\vec{F_R} = \frac{d\delta L_R}{dm} \tag{3.13}$$

For the radiative transfer the radiative luminosity L_R can be obtained from the radiative equilibrium condition;

$$L_R = -\frac{dT}{dr}\frac{16\pi acT^3}{3\kappa\rho}r^2 \tag{3.14}$$

Taking the logarithmic derivative of L_R;

$$\frac{\delta L_R}{L_R} = \frac{3\delta T}{T} + \frac{2\delta r}{r} - \frac{\delta\rho}{\rho} - \frac{\delta\kappa}{\kappa} + \frac{\delta(dT/dr)}{dT/dr} \tag{3.15}$$

First three terms have already been obtained from previous computations. The fourth term $\delta\kappa/\kappa$ is simply the opacity perturbation.

$$\frac{\delta\kappa}{\kappa} = \kappa_T\frac{\delta T}{T} + \kappa_\rho\frac{\delta\rho}{\rho} \tag{3.16}$$

where $\kappa_\rho$and κ_T are defined by:

$$\kappa_\rho = (\frac{\partial lnP}{\partial ln\rho})_T, \qquad \kappa_T = (\frac{\partial lnP}{\partial lnT})_\rho \tag{3.17}$$

Finally the last term can be derived as;

$$\frac{\delta(dT/dr)}{dT/dr} = \frac{\delta(\rho r^2 dT/dm)}{\rho r^2 dt/dm} = \frac{2\delta r}{r} + \frac{d\delta T/dr}{dT/dr} \tag{3.18}$$

where,

$$\begin{aligned} \frac{d\delta T/dr}{dT/dr} &= \frac{1/T(d\delta T/dr)}{1/T(dT/dr)} = \frac{\frac{d}{dr}(\delta T/T)}{1/T(dT/dr)} - \frac{\delta T \frac{d}{dr}(1/T)}{1/T(dT/dr)} \\ &= \frac{\frac{d}{dr}(\delta T/T)}{1/T(dT/dr)} + \frac{\delta T}{T} \end{aligned} \tag{3.19}$$

inserting this into Eq:

$$\frac{\delta(dT/dr)}{dT/dr} = \frac{2\delta r}{r} + \frac{\frac{d}{dr}(\delta T/T)}{1/T(dT/dr)} + \frac{\delta T}{T} \tag{3.20}$$

A star is vibrationally unstable towards the k-mode of oscillation if,

$$\int_0^M (\frac{\delta T}{T})_k (\delta\epsilon - \frac{d\delta L(r)}{dm(r)}) dm > 0 \tag{3.21}$$

Since ϵ does always increase with increasing ρ and T, $\delta\epsilon$ will be of the same sign as δT and the first term of the integral will always contribute to the instability.

If the heat capacity of the external layers is small, $\delta L(r)$ remains everywhere in phase with δT and for all ordinary opacity laws, the main term in $[\delta L(r)]/dm$ is proportional to $d(\delta T/T)/dm$. Thus the second part of the integral will always be negative and contribute to the stability.

Furthermore, the first part of the integral can be limited to the region where the generation of energy takes place, that is, close to the center where the amplitudes $\delta\rho/\rho$, $\delta T/T$ are small. The second part gets its main contribution from the external layers where the amplitudes are large. As Cowling (1936) first to show, this makes ordinary stars extremely stable.

Meanwhile, although no energy generation, only the opacity perturbation in PMS stars may be enough to make the second term to destabilize itself.

To investigate the influence of opacity on instability, a rough approximation can be applied with considering the strong dependence of behaviour of $\delta L/L$ on $\delta T/T$. This dependence has also been observed on the plots of models we had studied. Then the mass derivative can be written:

$$\frac{d\delta L_R}{dm} \propto L_R \frac{d\delta T/T}{dm} \tag{3.22}$$

Assuming a non-ionizing ideal gas with $\Gamma_3 = 5/3$ and no energy generation, since the mass gradient of δT is positive upon adiabatic compression, the absolute values of the variations in radius or density are small near the center and increase outward.

Equation (3.22) then implies that the mass gradient of δL_R is also positive on compression in this case of Krammer's opacity. $\partial \delta L_R/\partial m > 0$ upon compression means more radiative power leaks out of a mass shell than is entering. Thus the mass shell losses energy when compressed which is the criteria for stability.

If, on the other hand, we are in an active ionization zone where Γ_3 is less than 5/3, the mass gradient of δL_R can be negative when δT is positive. This

simply means a mass element gains heat upon compression and this leads to destabilization. Destabilization due to opacity is caused by the result of increasing opacity.

The value of κ_T increases in the inner part of an ionization zone and decreases in the outer part. Therefore, remembering equation (2.3), the excitation and damping zones due to the κ-mechanisms are located in, respectively the inner and outer parts of the ionization zone. Also the variation of $\Gamma_3 - 1$ enhances the excitation and damping effects due to the opacity derivatives.

In many cases an ionization zone exist in a convective zone. Although the general damping characteristics of these regions, excitation zone may extend into the upper layers of the ionization zone since the radiative luminosity gradient $\delta dL_r/dr$, is positive due to the convective energy flux decrease. These results may strongly be affected by convection-oscillation coupling.

3.2 Effect of Gravitational Contraction

Gravitational contraction means compression of star's fluid till a hydrostatic equilibrium is reached. A larger hydrodynamic system turns out te be a smaller one but with a more internal energy per unit. In other words, not as strong as a nuclear generation, but a continuous energy generation due to the gravitational contraction is provided. Increasing variables like pressure, temperature, etc. leads to the increase of their variations δp,δT.

According to Kato and Unno (1967), the excitation due to the gravitational

energy cannot be correctly treated if the dependence of ϵ_g on the physical quantities is assumed to be the same in the pulsating state as in the quasi-static state.

The overall effect of gravitational contraction on the work integral is given as:

$$W_g = \int_0^M (\frac{\delta T}{T})\delta\epsilon_g dM_r \tag{3.23}$$

and can be divided into two parts W_1 and W_2 where the latter is the effect due to the gravitational contraction coupling. Each is given as:

$$W_1 = 4\pi(\gamma-1)^2 \int_0^R \epsilon_g(3\xi + r\frac{d\xi}{dr})^2\rho_0 r^2 dr, \tag{3.24}$$

$$W_2 = 4\pi(\gamma-1)\int_0^R \epsilon_g[\frac{2}{3\gamma-4}(r\frac{d\xi}{dr})^2 + \frac{1}{2}(3\xi + r\frac{d\xi}{dr})^2]\rho_0 r^2 dr \tag{3.25}$$

respectively.

If we use $\delta\epsilon_g = (\frac{\delta T}{T})\epsilon_g$ in equation (3.23), we ignore the pulsation-contraction coupling, so the term W_2. Therefore the excitation in this case is more efficient than that when the coupling is neglected, by a factor somewhat larger than $(2\gamma-1)/2(\gamma-1)$

Gravitational contraction has a destabilizing effect with an opposite sign of the flux term in the work integral expression.

CHAPTER 4

MODELS

In our study we have investigated the models which have not finished their PMS evolution in the name of studying their vibrational properties. They are assumed to be in quasi-hydrostatic equilibrium during pre-main sequence phase and the evolution is governed by the rate of energy released from the gravitational contraction.

The models have chosen to be at the latest phases of the PMS evolution, between the bottom of the Hayashi track and ZAMS.

Evolutionary studies are started from the threshold of stability, while the models are on the Hayashi track, in a fully convective stage as in the work of Ezer and Cameron (1965). Collapsing protostar becomes stable against further dynamical collapse at the threshold of stability, at which the released gravitational potential energy of the star is just sufficient to supply the thermal, dissociation and the ionization energies of the models.

The stellar evolutionary code used in this study was described in Yildiz & Kiziloglu (1997) which is a modified version of Ezer's stellar evolutionary code

(Ezer & Cameron 1967). OPAL opacity tables (Iglesias et al 1992) were used together with the Alexander & Ferguson (1994) opacities for low temperatures.

MHD equation of state was applied to the stellar models (Mihalas et al 1990). Other details can be found in Yildiz & Kiziloglu (1997).

Evolutionary models of 1.5 ,2 ,2.5 ,3 ,3.5 and $4M_{\odot}$ stars have been studied with initial compositions, X=0.70, Y=0.28 Z=0.02 and the mixing length parameter $\alpha = 1.75$. The evolutions of these stars were followed through the pre-main sequence phase, where the evolution is governed by the rate of gravitational contraction energy released and of internal energy of the star.

CHAPTER 5

$3M_{\odot}$ RESULTS

In this chapter, the reader will be presented the results and discussions of $3M_{\odot}$ models' pulsational properties and vibrational stability characteristics.

With numerical computation of the linearized equations under the assumption of adiabatic approximation, we have obtained the eigenfunctions $(\delta r/r, \delta p/p)$ and the corresponding eigenvalues w^2 of the possible pulsating pre-main sequence δ-Scuti models and using adiabatic solutions, growth rates were calculated for stability analysis.

The ages of the investigated models were selected in the time interval between 2.6x10^6 and 3x10^6 years. This selection was made to be in harmony with the instability strip of Marconi & Palla (1998). In the evolutionary history of the model, this time corresponds to the region in the H-R diagram where the radiative zone is about to reach to the surface of the star and can be seen in Figure 1.1 as the "radiative-convective" region.

Basic characteristics and radiative region ratios of the $3M_{\odot}$ models are given in the Table 5.1. Massive and radial proportions of the radiative regions are also

Table 5.1: Basic evolutionary properties of the investigated 3Msun models

model	Te(K)	$L/L_{\odot}$	age(yrs)	$R/R\odot$	X_{rad}	R_{rad}
29	5884	32.87	2.638X10^6	5.600	0.9987	0.853
30	5940	35.07	2.679X10^6	5.600	0.9994	0.870
31	5997	37.08	2.720X10^6	5.649	0.9998	0.894
32	6063	39.42	2.716X10^6	5.698	0.9999	0.919
33	6107	40.76	2.782X10^6	5.711	0.9999	0.930
34	6157	42.06	2.802X10^6	5.707	0.9999	0.947
35	6215	43.44	2.822X10^6	5.694	1.0000	0.966
36	6282	44.89	2.843X10^6	5.665	1.0000	0.978
37	6286	44.99	2.844X10^6	5.663	1.0000	0.978
38	6293	45.12	2.846X10^6	5.659	1.0000	0.979
39	6309	45.45	2.850X10^6	5.651	1.0000	0.980
40	6339	46.02	2.858X10^6	5.633	1.0000	0.983
41	6358	46.40	2.863X10^6	5.622	1.0000	0.984
42	6443	47.98	2.884X10^6	5.567	1.0000	0.987
43	6622	51.17	2.925X10^6	5.442	1.0000	0.993
44	6986	57.69	3.007X10^6	5.193	1.0000	0.995

given in the last two columns of the table as $X_{rad} = m_{rad}/M$ and $R_{rad} = r_{rad}/R$ respectively.

Propagation diagram, that is the plot of dimensionless frequency, $w^2 = \sigma^2 R^3/GM$ versus radial displacement is plotted in Figure 5.1 for Model 41. Since we are dealing with radial oscillations (l=0), no Lamb frequency is found in the medium. This can also be seen in equation (2.1). After stability analysis which will be mentioned later, this model is found to be the last unstable model over the fundamental mode. Meanwhile the overtones are all stable. It can be noticed that the Brunt-Vaisala frequency is found even in the layers very close to the center since the inner convective region has not been extended enough. The frequency of the modes and the location of their nodes are also shown in the diagram. The model is oscillating in the fundamental mode with the dimensionless frequency $w^2 = 11.2400$ and as we go to higher p-modes, frequencies are increasing as well. Since there is no g-modes, we have no chance to observe a node in fundamental mode.

Figure 5.2 represents the evolution of dimensionless frequency of the investigated models for the fundamental and first three overtones. As seen in the figure, as the model evolves, while fundamental mode (f_0) and first overtone (p_1) have an increasing, second and third overtones have a decreasing trend till Model 36 with $T_{eff} = 6282$K which is the first model to have secured stability in p_3 mode after instability. After 6282K a constant attitude is followed. These gradual changes may be related to the change in the displacement of the nodes in the zone of continuously varying chemical composition in the models, as they evolve.

Mode bumping is a commonly encountered process in which discrete modes intersect with each other causing abrupt changes in frequency of oscillation. But

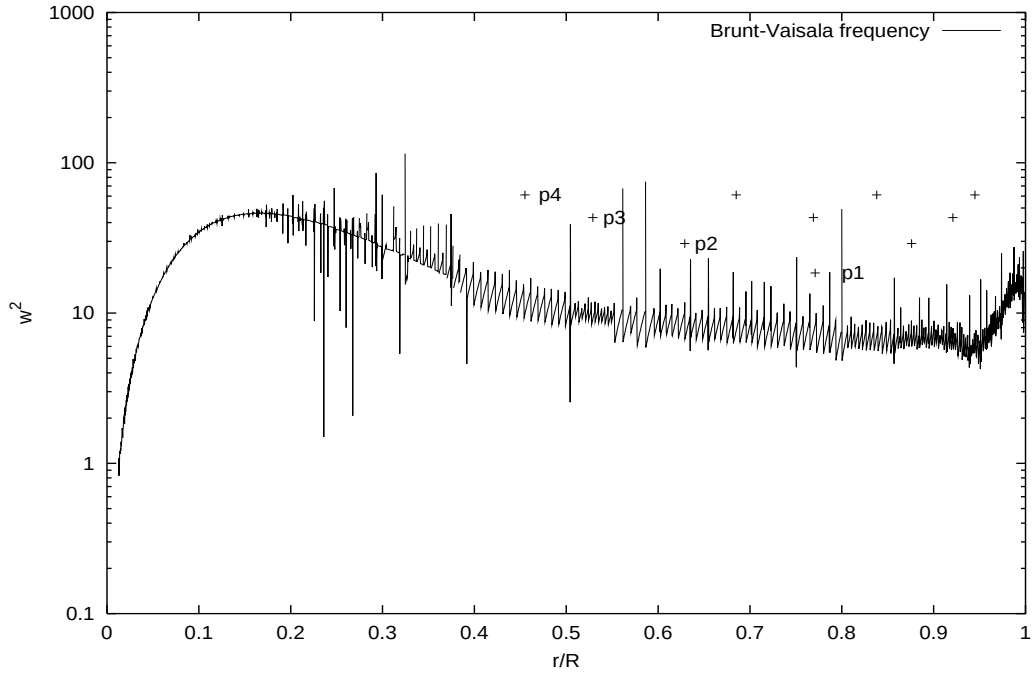

Figure 5.1: Propagation diagram for Model 41

our models are not sufficient to make prediction about possible mode bumpings. Moreover it is a process encountered at the very late stages of the stars.

Figure 5.3 and 5.4 demonstrate the behavior of the variations on radial displacement and pressure respectively. As expected, the curves intersect with the $\delta r = 0$ line, once for the 1st overtone and twice for the 2nd overtone. Fundamental mode oscillates with a frequency of 3.85 c/d (cycle/day), 1st overtone with 4.94 c/d and 2nd overtone with 6.18 c/d. Because regions being compressed during oscillation (negative δr) means increasing pressure (positive δp) and vice versa, $\delta r/r$ and $\delta p/p$ are upside down for the same modes.

One thing should be kept in mind during exploring this study and results that

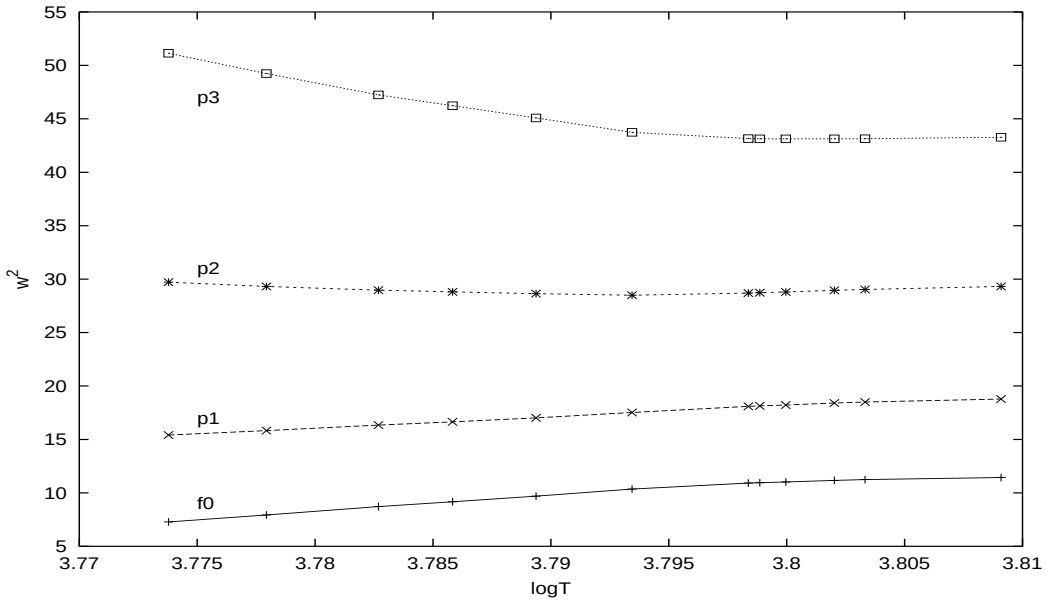

Figure 5.2: Evolution of dimensionless frequency for $3M_{\odot}$ models

we have limited all our calculations up to the end of the radiative region since we did not include the contribution of convective luminosity to the total luminosity because convective region of the outer envelope behaves non-adiabatic and all our approximations were adiabatic. For example all the plots of the present model (Model 41) are exhibited with ranges 0 to 0.984 which are the boundaries of the adiabatic radiative zone.

$\delta r/r$ and $\delta p/p$ plots roughly tell us that outer envelopes are more sensitive to the oscillations than the central regions with remarkable amplitudes.

κ-mechanisms at the outer envelopes are expected to be responsible for the instabilities in pre-main sequence stars since perturbation by $\epsilon - mechanism$ is improbable in such stars. This becomes clearer in the discussions of the $\delta\kappa/\kappa$ and

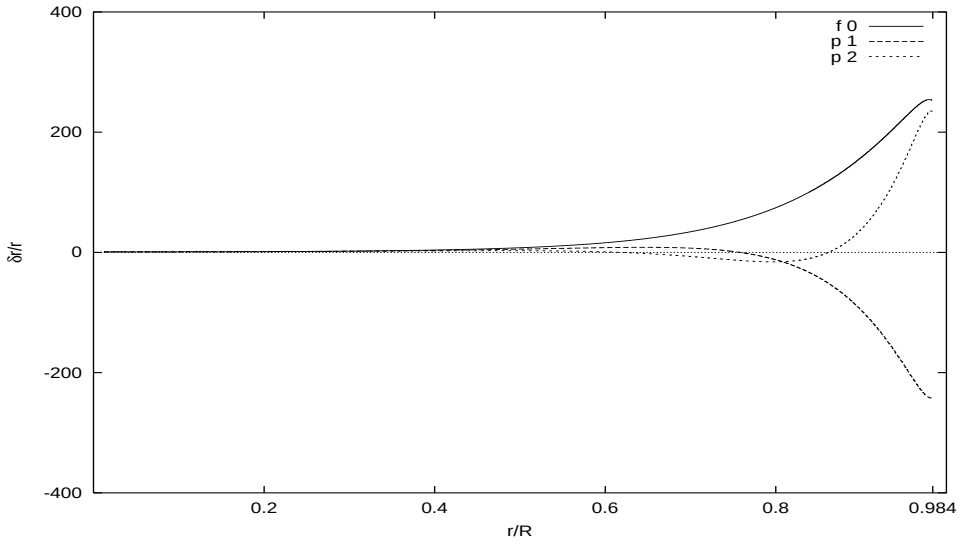

Figure 5.3: Lagrangian perturbation of radial displacement, $\delta r/r$ for f0, p1, p2 modes of $3M_{\odot}$ model

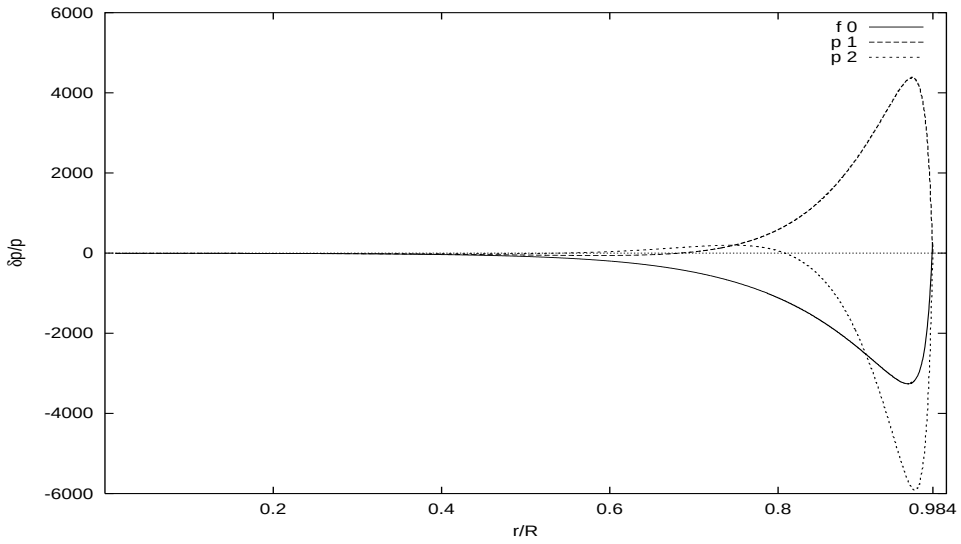

Figure 5.4: Lagrangian perturbation of pressure, $\delta p/p$ for f0, p1, p2 modes of $3M_{\odot}$ model

$\delta L/L$ plots which are given in Figures 5.5 and 5.6 respectively.

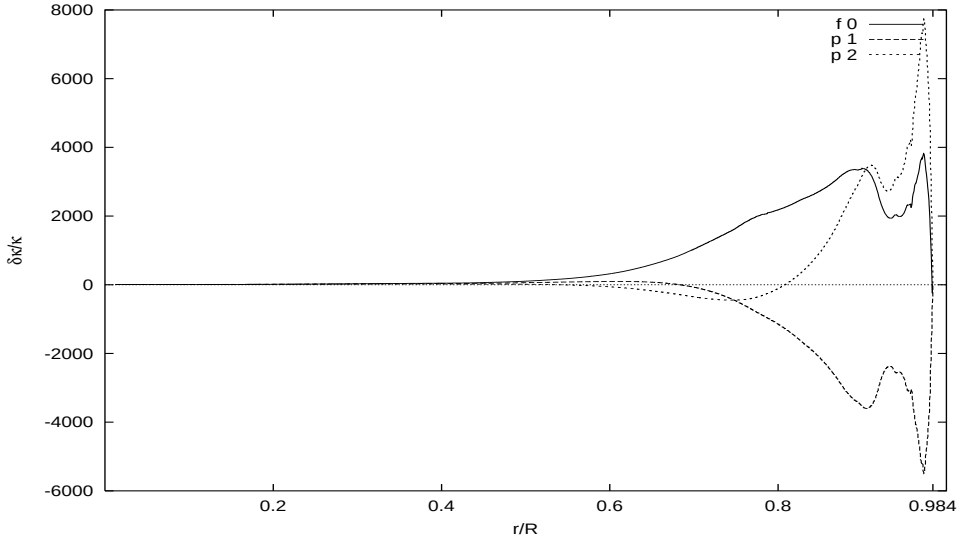

Figure 5.5: Lagrangian perturbation of opacity, $\delta\kappa/\kappa$ for f0, p1, p2 modes of $3M_{\odot}$ model

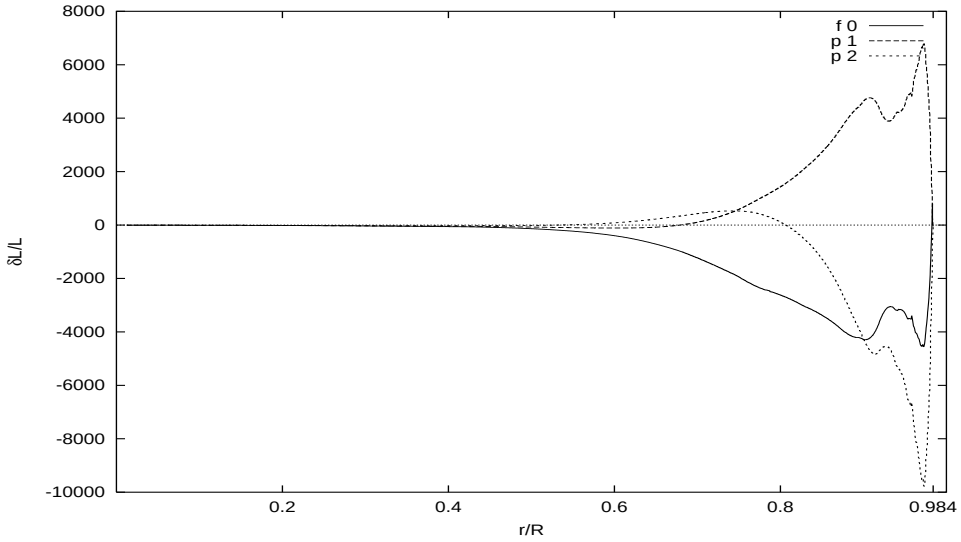

Figure 5.6: Lagrangian perturbation of luminosity, $\delta L/L$ for f0, p1, p2 modes of $3M_{\odot}$ model

A deformation is seen on the variation of opacity $\delta\kappa/\kappa$ at the outer layers of the star. This is a valuable confirmation to our rough prediction about how the instabilities occur. As expected κ-mechanism of the outer envelope would be responsible for the instability of our models.

Strong dependence of $\delta L/L$ on $\delta\kappa/\kappa$ is seen in these figures. Behavior of these curves are very similar and all the increments and decays match to the same radial displacements (r/R). Only the sign phase between these plots of the same modes are reversed which can be understood with the relation in equation (3.15).

The positions where $\delta L/L$ drops while $\delta p/p$ increases, are the most possible destabilizing regions of the star. This is because there is a tendency to keep the outgoing radiation energy, while compression takes place due to oscillation.

5.1 The Effect of Ionization

The goal is now to find out which relatively opac regions run the κ-mechanism to cause such instabilities. It is quite necessary to relate opacity distribution and development of growth rate (σ') that determines stability and computed shell by shell.

Figure 5.7 (κ vs T) shows how opacity changes and where the ionization zones are located. Ionization zones are easily distinguished in this plot since we know that ionization feeds opacity. Specifically, the partial ionization of He^+ ($He^+ \rightleftharpoons He^{++}$) is the main agent responsible for the pulsations in most common types of variable stars (Cox, J.,1980)

Every ionization zone appears at characteristic temperatures. These are roughly

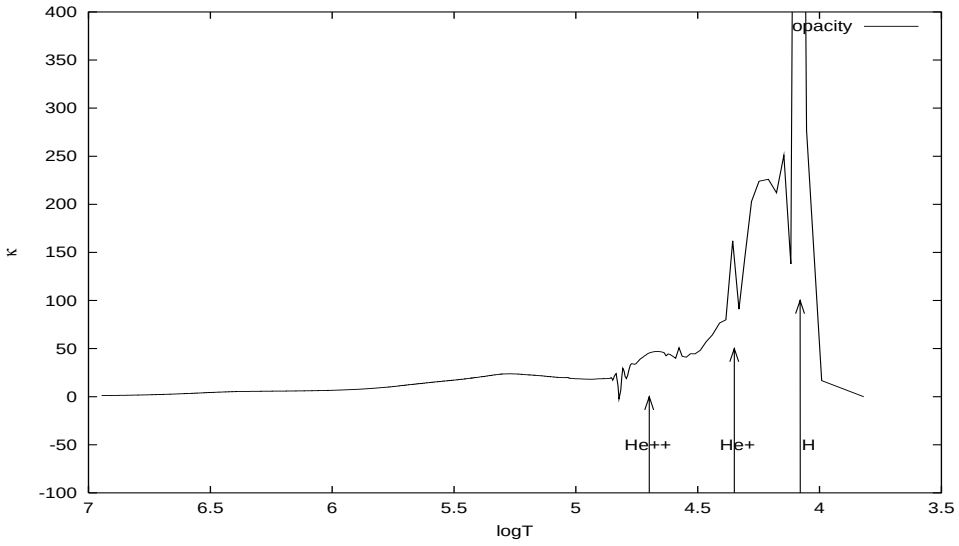

Figure 5.7: Opacity variation together with the ionization zones of the $3M_{\odot}$ model

1.2x10^4 K for H, 2.2x10^4 K for the first ionization of He (He^+) and 5x10^4 K for the second ionization of He (He^{++}) (R. F. Stellingwerf, 1979). These values also fit to the opacity bumping regions in our models (see Figure 5.7).

Stellingwerf suggests approximately six of these opacity bumping regions in every star, mostly formed by the H and He ionization zones, some by mixing of these two zones and some by heavy elements. The region between H and He bumpings in Figure 5.7 may possibly be the one of those mixing regions.

When the star takes breath in during oscillation, most of the work of adiabatic compression in these bumps goes into ionization energy rather than into kinetic energy of the thermal motion, so that the temperature does not increase very much upon compression.

In such a zone ($\Gamma_3 - 1$) becomes rather small as slightly did at the temperatures

corresponding to our He^{++} ionization zone. This leads to a mark dip for $(\delta L/L)$ since there is a strong sensitivity to $(\Gamma_3 - 1)$ as Cox suggested. Hence the flow of radiation is locally diminished. This favors destabilization.

We should take into account the position we had limited our calculations to clear out non-adiabatic effects. It corresponds to a temperature of about 6x10^4 K. Thus, only the second Helium ionization zone has the chance to fall into our adiabatic limits and most probably responsible for the instability.

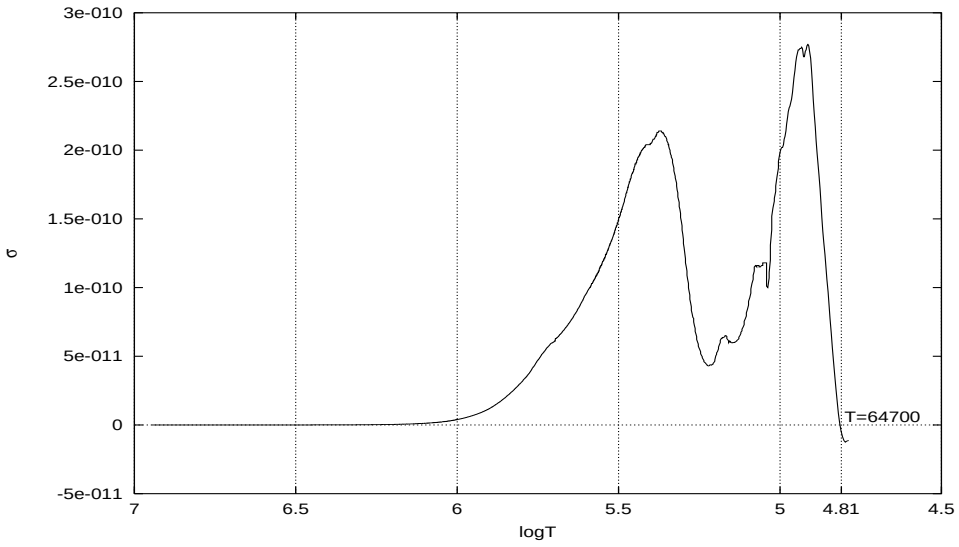

Figure 5.8: Growth rate of the fundamental mode of $3M_\odot$ model

In Figure 5.8 growth rate of fundamental mode for Model 41 is given. If at any point, the curve is above the horizontal axis, the star (from center to that point) is stable, otherwise unstable. Thus ascending parts stabilize, descending parts destabilize pulsation.

Two negative sloped region are seen in the figure; one results with a dip at

about log T=5.2, other with log T=4.8. The latter corresponds to He^{++} ionization zone while the former is a specific situation corresponding to the smooth peak on the left of He++ zone on Figure 5.7.

Stellingwerf (1979) had explained this zone as a driving region that corresponds to the photon energy peak in the radiation peak (at 1.5x10^5 K). This effect is referred as "bump mechanism".

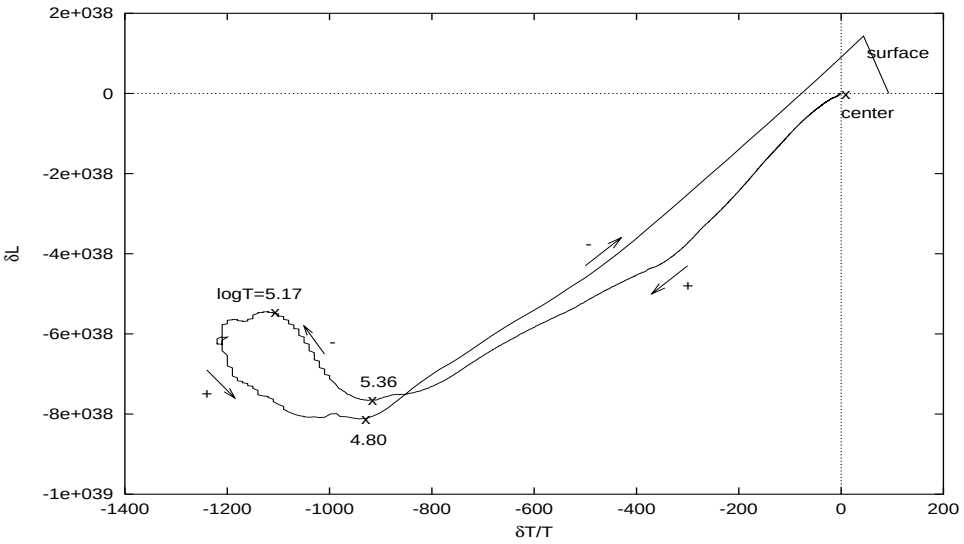

Figure 5.9: δL as a function of $\delta T/T$ for f0 mode of $3M_{\odot}$ model

δL vs $\frac{\delta T}{T}$ curve, presented in Figure 5.9, is another useful tool to examine stability characteristic and driving and damping regions of the star. Since stability analysis is based on the integration of $(\delta L.\frac{\delta T}{T})$ product.

Positive and negative contributing regions are shown in Figure 5.9. Regions having positive $(\delta L.\frac{\delta T}{T})$ product are damping pulsation, while negative products are driving.

Two driving regions between log T=(5.36-5.17) and log T=(4.9-4.8(surface)) are noticed which entirely corresponds to negative sloped regions of σ' curve. Thus we have surely figured out the driving and damping regions of the star.

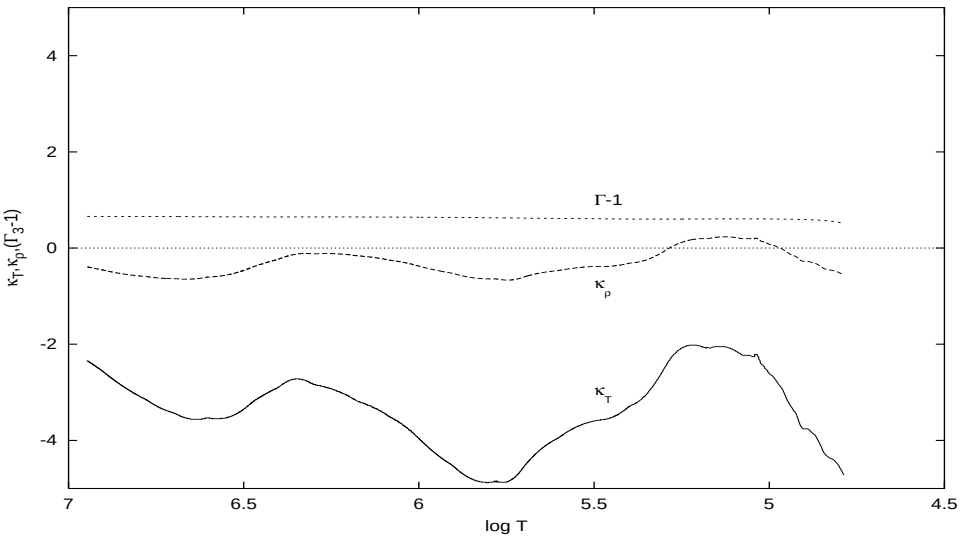

Figure 5.10: $\Gamma_3 - 1$, κ_T and κ_ρ for f0 mode of $3M_\odot$ model

In Figure 5.10 variations of opacity derivatives and $(\Gamma_3 - 1)$ are shown together. It is seen that κ_T is the most effective factor in the analysis of criterion in equation (2.3) and thus it seems to be the most effective component of κ-mechanism on exciting the oscillation.

5.2 Instability Period

Models tested for stability, were found to have lived an instability period of $0.167\text{x}10^6$ years for $3M_\odot$. All the instabilities of the unstable models come from the κ-mechanism of the outer envelopes as it is in Model 41 which had been

investigated in previous sections.

Table 5.2 shows how vibrational stability of a $3M_{\odot}$ PMS star evolves. Fundamental modes and first three overtones are shown in the Table. We see from the Table that instability starts from higher overtones to lower ones just as re-stability does. (+) refers to "stable model" while (-) refers to "unstable model".

Table 5.2: Results of stability analysis of $3M_{\odot}$

model	Te	age(yrs)	f0	p1	p2	p3
29	5884	$2.638\text{X}10^6$	+	+	+	-
30	5940	$2.679\text{X}10^6$	+	+	-	-
31	5997	$2.720\text{X}10^6$	+	-	-	-
32	6063	$2.716\text{X}10^6$	-	-	-	-
33	6107	$2.782\text{X}10^6$	-	-	-	-
34	6157	$2.802\text{X}10^6$	-	-	-	-
35	6215	$2.822\text{X}10^6$	-	-	-	-
36	6282	$2.843\text{X}10^6$	-	-	-	-
37	6286	$2.844\text{X}10^6$	-	-	-	-
38	6293	$2.846\text{X}10^6$	-	-	-	-
39	6309	$2.850\text{X}10^6$	-	-	-	+
40	6339	$2.858\text{X}10^6$	-	-	+	+
41	6358	$2.863\text{X}10^6$	-	+	+	+
42	6443	$2.884\text{X}10^6$	+	+	+	+
43	6622	$2.925\text{X}10^6$	+	+	+	+
44	6986	$3.007\text{X}10^6$	+	+	+	+

CHAPTER 6

INSTABILITY STRIP

One of the most remarkable results of this study was that the pre-main sequence stars pass through a period where the fundamental and lower p-modes are unstable for radial oscillations. As mentioned in the first chapter, this was already studied by a number of scientists both observationally and theoretically. Marconi M. & Palla F. (1998) was the most well-known because of the accurate results and as being the first theorotical study.

Marconi and Palla (1998) had studied vibrational instability of 1.5-4$M\odot$ pre-main sequence stars for radial adiabatic pulsations and suggested an instability strip for the first three radial modes. Time spent by the star during crossing this region is very small compared to post-ZAMS cases. This reduces the chance to catch a star in this phase of evolution. Inspite of this handicap, many pre-main sequence variables were observed to be crossing this strip. This has also stiffen the reliability of their study.

We expanded our stability analysis for 2, 2.5, 3, 3.5 and 4$M\odot$ models to figure out the instability strip formed after adiabatic computation of PMS models. Thus

we would also able to compare our results with those of Marconi and Palla (1998).

The strip is figured between the time the fundamental mode becomes first unstable for the first time and the time the same mode leaves instability region. The results can be seen in Figure 6.1 where Marconi and Palla (1998) instability region is also shown.

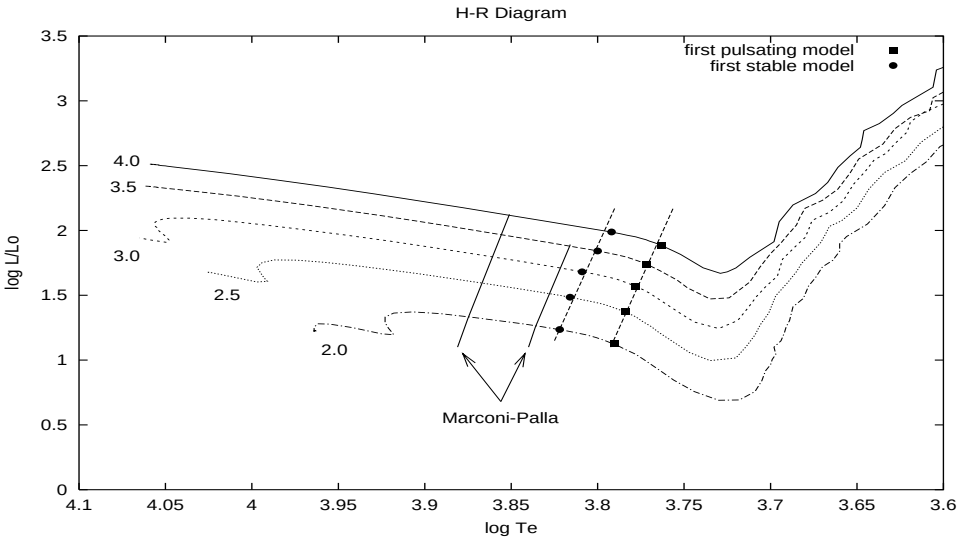

Figure 6.1: Instability strip for the 2, 2.5, 3, 3.5, $4M_{\odot}$ models

As given in Table 5.1 the redder the models, the larger the non-adiabatic convective envelopes are found within the star. Thus since we deal only with adiabatic parts, the degree of accuracy decreases as we approach to the red boundary of the strip.

In Table 6.1, the boundary properties are given. As seen in the table, the red edge varies between 5795 K and 6165 K whereas the blue edge varies between 6196 K and 6649 K. These values are much cooler than the results of Marconi

Table 6.1: Properties of the models on edges of the instability strip

	RED EDGE			BLUE EDGE		
$M/M_{\odot}$	$L/L_{\odot}$	T_{eff}	age(yrs)	$L_{\odot}$	T_{eff}	age(yrs)
2	13.55	6165	$9.406\text{X}10^{6}$	17.22	6649	$9.693\text{X}10^{6}$
2.5	23.53	6087	$4.662\text{X}10^{6}$	30.56	6550	$4.908\text{X}10^{6}$
3	37.08	5997	$2.720\text{X}10^{6}$	47.98	6443	$2.884\text{X}10^{6}$
3.5	54.86	5909	$1.604\text{X}10^{6}$	69.47	6309	$1.717\text{X}10^{6}$
4	76.54	5795	$1.061\text{X}10^{6}$	97.22	6196	$1.153\text{X}10^{6}$

and Palla (1998) as can also be seen in the Figure 6.1. This might have number of reasons some of which will be discussed in the next paragraphs.

The avarage width of the strip is about 450 K and the duration of the models on the strip varies between 0.287 million years for $2M_{\odot}$ and 0.092 million years for $4M_{\odot}$ which is proportional to their PMS contraction phase.

The main reason for the difference between the boundaries of the strip that we have computed, and Marconi & Palla did, is that the input physics adopted in this study is entirely different from the input physics that they used in their study. They used models computed by Palla & Stahler (1993) which involved Roseland Mean Opacities and equation of state, taking the ratio of mixing length to pressure scale height as α=1.5. We used OPAL opacities (Iglesias et al., 1992), MHD equation of state and α is taken as 1.75. Their models were starting at the birthline where the stars are fully radiative for masses $\geq 2.5M_{\odot}$ while our models begin at the threshold of stability at which the gravitational potential energy of the contracting protostar becomes just greater than the sum of the thermal, dissociation and ionization energies of the gas.

When we compare the ZAMS temperatures, we see that their ZAMS temperatures are much larger than ours although initial temperatures are almost the same. Thus our evolutionary tracks show a shift to the right in the H-R Diagram with respect to theirs.

The shift in our evolutionary tracks to the right bottom, possibly might have given rise to the shift of the instability strip during the PMS phase.

PMS models were computed starting at the birthline which is determined

by the protostellar accretion phase. The protostellar mass-radius relation gives directly the starting radii for PMS contraction. Deterium burning plays an important role in determining the protostar radius. If the energy per unit time released by the fusion of deterium to helium $[H(p,\gamma)He^3]$, exceeds the radiative luminosity, star is convectively unstable that occurs for masses less than $2.44M_\odot$ for an accretion rate of $10^{-5}M_\odot yr^{-1}$. $2M_\odot$ star contracts for only 1.1x10^4 years before a radiative core appears at the center. In our models radiative core appears after 1.5x10^5 years.

Deuterium burning extends the contraction time of the lower mass stars particularly. Low mass stars are too cold to ignite deuterium during accretion (Stahler et al., 1980). Palla & Stahler concluded that for intermediate mass stars the deuterium supply is limited because of prior protostellar consumption, and the effect of deuterium burning is diminished on the subsequent contraction for 1.5 and $2M_\odot$ stars. In their study, the star becomes fully radiative at 9.43x10^6 and 3.36x10^6 years. But in our study, stars have a convective outer zone as they evolve to the ZAMS. This phenomenon may be another considerable effect on the shifting of the results.

6.1 Frozen Convection

During this study, a difficulty in treating perturbation of energy flux has been faced. Actually, energy flux consists of radiative and convective flux components. Treatment of these perturbations contains adiabatic parameters and it would be incorrect to apply them at the non-adiabatic convective outer envelope of a star.

In the times when the convection theory had not been developed an approximation called "frozen convection" used to be applied to get rid of this problem which neglects the convective flux perturbation and equalize the total flux perturbation to radiative flux perturbation.

In this manner we studied frozen convection to see how it would effect the results. This time we had included the convective envelope into our computations and used radiative luminosity perturbation from center upto the surface.

All the models were run again with this approximation and the new instability strip was drawn as in Figure 6.2.

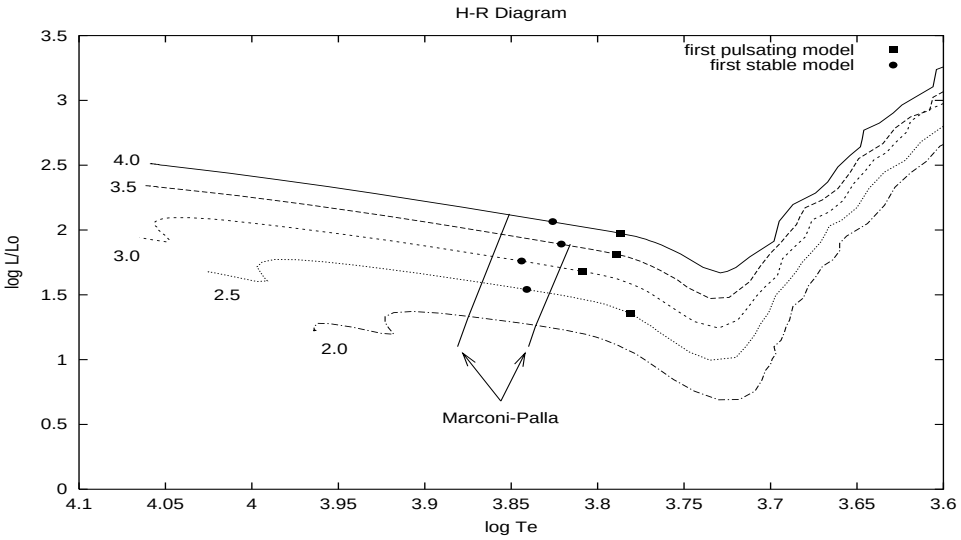

Figure 6.2: Instability strip for the 2, 2.5, 3, 3.5, $4M_{\odot}$ models with the frozen convection approximation

Instability strip for $2M\odot$ has not been drawn because of the distrustful results in this mass. When compared with the results in the previous section (see Figure

6.1), boundaries of the instability strip seem to be placed closer to the boundaries of Marconi & Palla (1998). Moreover some parts of the strips intersect with each other. But the bothersome things are these distrustful results, disordered borders and the imbalance in the duration period on the strip for different masses.

6.2 Gravitational Contraction

Since the investigated models are at the latest phases of the gravitational contraction, we should examine if there is a significant impact of contraction upon oscillation of these models.

As mentioned before, the effect of gravitational contraction on pulsation is towards destabilization. In Table 6.2 the effect of gravitational contraction on vibrational instability is demonstrated in terms of the growth rate. The gravitational energy generation term $E_g = W_g/E_W$ and the flux term $E_F = W_F/E_W$ are given in the Table where W_g is given in equation (3.23), E_W in equation (3.5) and W_F in equation (3.13).

The effect of the gravitational contraction term is significant in the deeper layers. For example, at the center it is 0.28 times the flux term. But when closing to the surface where the oscillation amplitude is appreciable this effect is losing its importance and becomes 0.001 times the flux term. Thus the overall effect of gravitational contraction to the σ' value is found to be very small and is negligible.

Table 6.2: The weight of the gravitation and flux terms on the growth rate

X [r/R]	E_F	E_g	σ'
0.015	$0.126\text{x}10^{-17}$	$0.342\text{x}10^{-18}$	$0.918\text{x}10^{-18}$
0.200	$0.469\text{x}10^{-14}$	$0.737\text{x}10^{-15}$	$0.395\text{x}10^{-14}$
0.400	$0.421\text{x}10^{-13}$	$0.236\text{x}10^{-14}$	$0.397\text{x}10^{-13}$
0.600	$0.658\text{x}10^{-12}$	$0.402\text{x}10^{-14}$	$0.654\text{x}10^{-12}$
0.800	$0.145\text{x}10^{-10}$	$0.651\text{x}10^{-14}$	$0.395\text{x}10^{-10}$
1.000	$-0.869\text{x}10^{-11}$	$0.648\text{x}10^{-14}$	$-0.870\text{x}10^{-11}$

CHAPTER 7

CONCLUSION

In this study, pulsational properties of pre-main sequence stars in the mass range of 2-4M$\odot$ have been studied. The computation of the linear adiabatic radial oscilations of the models which have not completed their PMS evolution has been carried out with the oscillation program firstly written by Kırbıyık & Al-Murad (1993). Vibrational instability of the models were also investigated with some additions to the code and the results were compared with the previous studies on this subject.

The models were chosen at the latest phases of the PMS evolution where radiative regions are dominant in the star except the thin outer convective envelopes whose widths are changing due to how much they have evolved. The most serious difficulty we had faced during this study was the computation of these non-adiabatic convective envelopes.

The difficulty came in when we had to choose another approximation for the outer layers, since running the adiabatic computations for these non-adiabatic layers would be far from accuracy. In this way we had experienced two different

approximations:

First is to apply the computations only to the adiabatic part and investigate the pulsation phenomenon at this very large portion of the star. Inspite of incompleteness, this approach gave us a lot about the pulsation properties of PMS stars. How they are characterized, what excitation mechanisms are used, which parts of the star stabilize, which parts destabilize pulsations, etc..

The κ-mechanism was found to be completely responsible for the instability of pre-main sequence stars.In this mechanism, the energy flowing away from the star is blocked by some opaque parts. The excess energy in any layer may excite the star to pulsate. These layers of high opacity is formed when ionization occurs. Moreover, these regions of partial ionization were located in the outer layers where the pulsation amplitude is appreciable. In our PMS models it was found that the He^{++} ionization zone was the main responsible agent for exciting the pulsation.

Theoretical instability strip for the PMS pulsating stars had been drawn by Marconi & Palla (1998) for radial adiabatic pulsations. The strip that we formed from our analysis was observed to be shifting to the right with respect to their strip in the H-R Diagram. It was argued the shift might be due to the differences between the input physics. Not only the models were created with different methods, we also have an outer convective envelope for each model while their models were fully radiative. Besides our evolutionary tracks were already shifted. Thus, it may concluded that if the differences that we mentioned above between two treatments have been removed, we may obtain a matching strip.

Second approach used by us was the frozen convection where the radiative

luminosity perturbation was used all over the star. This time the instabilty strip intersects with the one in Marconi & Palla (1998). But the boundaries of the strip this time was quite random. This might be because the He^+ and H ionization zones that are very close to the surface and omitted in the previous approximation are setting in now.

A PMS δ-Scuti pulsation differs from the post-ZAMS one with the way it is excited. A Main Sequence δ-Scuti star may also be excited by the ϵ-mechanism. This changes all the oscillation characteristics. Inspite of this, the pulsation periods found were close to the MS pulsation periods.

One of the typical properties of the PMS stars is that they are in a gravitational contraction phase. Therefore, we also investigated how gravitational contraction effects pulsation. We found that the destabilizing effect of gravitational contraction is remarkable at the inner regions but neglegible at the outer envelopes where pulsation really does take place. Therefore the gravitational contraction can surely be omitted.

In fact, Isao Okamoto (1967) had suggested that the effect of gravitational contraction on pulsation was important in early PMS stars. But, since our models are in a region of H-R Diagram, very close to ZAMS where the degree of contraction is diminishing it is realistic to reach the conclusion that the gravitational contraction can be neglected.

During this study, we have neglected rotation, convection-pulsation and pulsation-contraction coupling for simplicity. Inclusion of these effects may be a subject of a future study.

On the other hand, the oscillation program should be updated for non-adiabatic treatments.

Addition of non-linear analysis will certainly lead us to more accurate results.

REFERENCES

[1] Alexander D. R., Ferguson C. W., 1994, ApJ, 437, 879

[2] Balona L. A., Koen C., van Wyk F., Ripepi V., 2002, MNRAS, 333, 923

[3] Baker N, Kippenhahn R., 1962, Z. Astrophys., 54, 114

[4] Baker N, Kippenhahn R., 1965, ApJ, 142, 868

[5] Boury A., et al., 1975, A&A 41, 279

[6] Breger M., 1972, ApJ, 171, 539

[7] Breger M., Pamyatnykh A.A., 1998, A&A, 332,958

[8] Breger M., 1972, ApJ, 171, 539

[9] Catala. C., 2003, Astrophysics and Space Science, 284, 53

[10] Cowling T. G., 1936, Astronomische Nachrichten, 258, 133

[11] Cowling T. G., 1941, Monthly Notices Roy. Astron. Soc., 101, 367

[12] Cox J. P., 1980, Theory of Stellar Pulsation, Princeton University

[13] Dalsgaard J. C., Dziembowski W. A., 2000, Variable Stars as essential Astrophysical Tools, v.1

[14] Donati J. F., Semel M., Carter B.D., et al., 1997, MNRAS, 291, 658

[15] Eddington A. S., 1926, The Internal Constitution of the Stars (Cambridge Univ. Press, Cambridge), p.198

[16] Ezer D. 1967, Margherita, 357

[17] Ezer D., Cameron A.G.W. 1962, Sky and Telescope, 24, 328

[18] Ezer D., Cameron A.G.W. 1965, Can. J. of Phys., 43, 1497

[19] Ezer D., Cameron A.G.W. 1966, Plenum Press, 203

[20] Ezer D., Cameron A.G.W. 1967, Can. J. of Phys., 45, 3461

[21] Gabriel M., Scuflaire R., Noels A., Boury A., 1975, A&A, 40, 33

[22] Guzik J.A. 2000, Variable Stars as essential Astrophysical Tools, 213

[23] Ibrahim A., Boury A., Noels A., 1981, A&A 103, 390

[24] Iglesias C. A., Rogers F. J., Wilson B. G., 1992, ApJ, 397, 717

[25] Kato S., Unno W. 1967, PASJ, 19, 1

[26] Kırbıyık H.,Al-Murad M.A., 1993, MS Thesis in Physics by Al-Murad M. A., Metu

[27] Kızıloglu N., Ezer D. 1982, Sun and Planetary System, 59

[28] Kızıloglu N., Kırbıyık H., Civelek R. 2000, Turkish Journal of Physics, 26, 185

[29] Kızıloglu N., Kırbıyık H., Civelek R. 2003, International Journal of Modern Physics D, 12, 1067

[30] Kurtz D. W., Marang F. 1995,Royal Astronomical Society, 276, 191

[31] Kurtz D. W., Muller M., 1999, MNRAS, 310, 1071

[32] Kurtz D. W., Muller M., 2001, MNRAS, 325, 1341

[33] Kurtz D.W., Catala C. 2001, A&A, 369, 981

[34] Ledoux P. 1957,International Astronomical Union. Symposium no.3, 186

[35] Ledoux P., Walvaren T., 1958, Handbuch der Physik, ed. S. Flugge, 51, 353

[36] Lee U. 1985, PASJ, 37, 279

[37] Marconi M., Palla F. 1998, ApJ, 507, L141

[38] Marconi M., Ripepi V., Alcala J. M., et al., 2000, A&A, 355, L35

[39] Marconi M., Ripepi V., Bernabei S., et al., 2001, A&A, 372, L21

[40] Mihalas D., Hummer D. G., Mihalas W., Dappen W., 1990, ApJ, 350, 300

[41] Okamoto I. 1967, PASJ, 19, 384

[42] Palla F., Stahler S.W. 1993, ApJ, 418, 414

[43] Pamyatnykh A.A. 2000, ASP Conferece Series, 210, 215

[44] Pinheiro F., Folha D., Monteiro M. J., et al., 2002, ASP Conferece Series, 259, 352

[45] Pigulski A., Kolackzkowski Z, Kopacki G, 2000, AcA, 50, 113

[46] Rodrigez E., Breger M. 2001, A&A 366, 178

[47] Stahler S. W., Shu F. H., Taam R. E., 1980, ApJ, 242, 226

[48] Stellingwerf R. F., 1979, ApJ, 227, 935

[49] Suran M., et al. 2001, A&A, 372, 233

[50] Unno W. 1967, PASJ, 19, 140

[51] Yıldız M., Kızıloglu N., 1997, A&A, 326, 187